Journal of Coastal and Ocean Sciences *e-issn: 2746-4512*
Volume 5 No. 1, January 2024: 17-26 *p-issn: 2745-4355*

Analysis of Wave Characteristic in Fuel Terminal Serui

Ahmad Azwar Mas'ud M[1*], Suntoyo[1], Widi A. Pratikto[1]
[1]Department of Ocean Engineering, Institut Teknologi Sepuluh Nopember, Surabaya 60111 Indonesia
Corresponding Author: ahmadazwarmasud@hotmail.com

Received: December 15, 2023; Accepted: January 5, 2024

ABSTRACT

The Serui Fuel Terminal is a vital state-owned facility distributing fuel oil throughout Yapen Island, Papua Province. However, this facility has a problem: waves or overtopping, which can even cause damage to existing facilities. This research aims to determine the hydrodynamic process and wave characteristics through theoretical analysis and numerical modeling using Mike21 with Hydrodynamic (HD) and Spectral Wave (SW) Modules. Bathymetry, current and tidal data collected in the field and wave data collected from ECMWF, calibration is carried out by comparing modeling output (currents & tides) with the results of observations and wave propagation and transformation study theoretically and compared with the results of wave modeling, so the accuracy of the modeling results can be reviewed. The validation results of tidal modeling with a MAPE (Mean Absolute Percentage Error) value of 0.3%, current modeling with a MAPE value of 30%, and waves from each orthogonal with an average MAPE of 15%. Generally, wave height on the shoreline is 0.3-0.4 m (calm waves), and the cause of the overtopping that occurs is due to the geometry and type of existing coastal buildings with smooth sloping sides and impermeable, which makes the wave height double with a run-up height 0.6-0.8 m.

Keywords: Hydrodynamics, Numerical Modelling, Run-Up, Wave Transformation

1. INTRODUCTION

The coastal area is an area that has both economic and tourism potential. The beach can be interpreted as an area where the land area meets the sea area. The beach is classified as an area or location where oceanic forces interact with the land (CERC, 1984). However, on the other hand, the beach also has problems, such as what happened in the Serui Fuel Terminal area, a facility owned by PT Pertamina (Persero) in the Yapen Islands Regency, Papua Province, namely, the problem of high waves in the Fuel Terminal area. Previously, there was an existing protective building in the form of a seawall, which was expected to protect the facility from wave problems. However, waves still overtopped the building, especially at high tide, where the tide in Yapen Waropen waters is approximately 2 m (Husrin and Prihantono, 2007), because the top of the building was relatively low from the tide level.

The building geometry was relatively vertical, which caused high wave run-up and overtopping. It is an important variable for designing coastal area defenses (Di Leo et al., 2022), even when combined with waves from another direction (Van der Werf and Van Gent, 2018). To determine the type of building and handling of a coastal problem, paying attention to water dynamic phenomena such as wave patterns is necessary. Waves are important because they are influenced by significant wave height, tidal rides, and wave transformation (Sugianto and Andika, 2015). Wave propagation, such as refraction and diffraction, must also be known, especially in planning port buildings (Amalia et al., 2014).

Figure 1. Overtopping of existing structures

However, it is necessary to study whether the wave energy in front of the building is still high if viewed from the convergent and divergent processes of the spread of wave energy when the wave breaks when it hits the building structure because of the morphological conditions. One approach to treat this problem is to apply wave models to

transform offshore wave directional spectra to inshore spectra and exploit the available geographical information (bathymetry, coastline) (Belibassakis et al., 2014) to evaluate wave transformation to the coast using spectral models such as SWAN and STWAVE (Rusu et al., 2011) and various spectral models with multiple conditions such as sheltered estuaries (Taylor-Burns et al., 2023), open bay (Rusu et al., 2011), coral reef (Mandlier and Kench, 2012) and various reef profiles (Fang et al., 2014), especially along buildings that are relatively deeper so that the wave energy is still high. It broke when it hit an existing building compared to its surroundings, greatly influencing the differences in wave transformation and current patterns in the Fuel Terminal area and its environs.

Numerical modeling can be carried out to examine the hydrodynamic behavior and nearshore morphology, allowing the study of interactions between different structures (Oliveira et al., 2018). Waves propagate from deep waters towards the shore through several processes of change in wave height, speed, direction, and other phenomena such as shallowing processes (wave shoaling), refraction processes (refraction), diffraction processes (diffraction), or reflection processes (reflection) before the wave broke (wave breaking) (Pratikto et al., 2014).

In this research, a numerical study and theoretical analysis of wave transformation will be carried out where validation is carried out on currents and tides and theoretical validation of waves due to the influence of shoaling and refraction based on the morphological conditions of the waters.

2. RESEARCH METHOD

Time and Place

Serui Fuel Terminal is in Yapen Island, Banawa, South Yapen, Yapen Islands Regency. The Serui Fuel Terminal location map can be seen as follows in Figure 1.

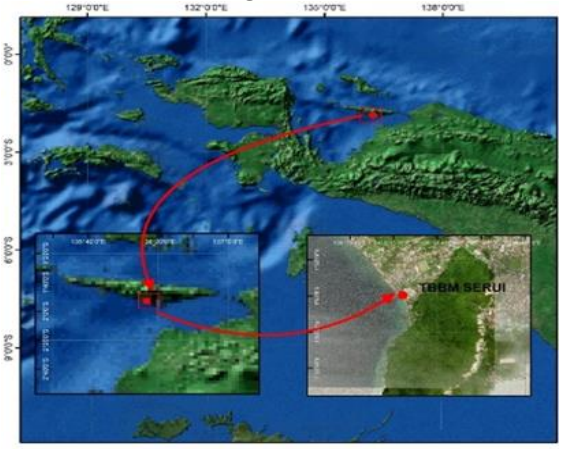

Figure 2. Fuel Terminal Serui location

Method

The research was carried out by collecting primary and secondary data, then doing theoretical wave transformation calculations, creating orthogonal wave lines, and determining reference points to validate wave, current, and tidal modeling. The data used can be seen in Table 1.

Table 1. Data used

No.	Description	Type Data	Amount data	Data source
1	Topografi-Bathimetry	Primary	-	Field Survey
		Secondary	-	Pushidros-AL/Navionics
2	Tides	Primary	15 Days	Field Survey
3	Current Data	Primary	15 Days	Field Survey
4	Significant -Waves (Hs)	Secondary	365 Days	ECMWF

Procedures

Hydrodynamic Modeling

The hydrodynamic model in the MIKE 21 Flow Model (MIKE 21 HD) is a general numerical model for simulating water levels and currents in estuaries, bays, and coastal areas. It simulates unsteady two-dimensional flows in one-layer (vertically homogeneous) fluids and has been applied in many studies. The following equations, the conservation of mass and momentum integrated over the vertical, describe the flow and water level variations (DHI, 2014).

$$\frac{\partial \zeta}{\partial t} + \frac{\partial p}{\partial x} + \frac{\partial q}{\partial y} = \frac{\partial d}{\partial t}$$

$$\frac{\partial p}{\partial t} + \frac{\partial}{\partial x}\left(\frac{p^2}{h}\right) + \frac{\partial}{\partial y}\left(\frac{pq}{h}\right) + gh\frac{\partial \zeta}{\partial x} + \frac{gp\sqrt{p^2+q^2}}{C^2.h^2} - \frac{1}{\rho_w}\left[\frac{\partial}{\partial x}(h\tau_{xx}) + \frac{\partial}{\partial y}(h\tau_{xx})\right] - \Omega_q - fVV_x + \frac{h}{\rho_w}\frac{\partial}{\partial x}(P_a) = 0$$

$$\frac{\partial q}{\partial t} + \frac{\partial}{\partial y}\left(\frac{q^2}{h}\right) + \frac{\partial}{\partial x}\left(\frac{pq}{h}\right) + gh\frac{\partial \zeta}{\partial y} + \frac{gp\sqrt{p^2+q^2}}{C^2.h^2} - \frac{1}{\rho_w}\left[\frac{\partial}{\partial y}(h\tau_{yy}) + \frac{\partial}{\partial x}(h\tau_{xy})\right] - \Omega_p - fVV_y + \frac{h}{\rho_w}\frac{\partial}{\partial xy}(P_a) = 0$$

Wave Modeling

MIKE 21 SW can be used for wave prediction and analysis on regional and local scales. MIKE 21 SW also uses sediment transport calculations, primarily determined by wave conditions and wave-induced currents. Wave-induced currents are caused by gradients of radiation stresses in the surf zone. MIKE 21 SW can be used to calculate wave conditions and radiation stresses. This module's governing equation is the wave force balance equation in Cartesian and spherical coordinates formulated by Komen et al. (1994) and Young (1999) (DHI, 2014).

Cartesian co-ordinates: $\frac{\partial N}{\partial t}+\nabla.(\vec{v}N)=\frac{S}{\sigma}$

Where N ($\vec{x}$, σ, θ, t) is action density, t is the time, $\vec{x}(x,y)$ is the Cartesian coordinates, $\vec{v}$ (cx, cy, cs, cθ) is the propagation velocity of wave group in the four-dimensional phase space. S is the source term for the energy balance equation.

Spherical coordinates: $\dot{N}=NR^2\cos\Phi=\frac{ER^2\cos\Phi}{\sigma}$

Where N ($\vec{x}$, σ, θ, t) is action density, $\vec{x}$ (ϕ,λ) is spherical coordinates, where ϕ is latitude and λ is longitude. E is normal energy density.

In the spectral wave module, the data used is wind or waves, bathymetry, and tidal data, and the result is radiation stress, which can be used for input data in modeling current patterns in the hydrodynamic module. Meanwhile, for the hydrodynamic module, the data used are wind, bathymetry, tidal, and radiation stress (wave radiation). The data that can be generated is current speed, current pattern, and surface elevation, then used for validation (Ghipari et al., 2012)

Validation

The validation value is based on the MAPE (Mean Absolute Percentage Error) value proposed by Lewis (1982), where the equation is as follows

$$MAPE = \frac{1}{n}\sum_{i=1}^{n}\left|\frac{actual-forecast}{actual}\right| x100$$

Where n is the amount of data, typical MAPE accuracy values for model validation can be seen in Table 2.

Table 2. Typical MAPE values in modeling validation

MAPE (%)	Forecasting Power
<10%	Highly accurate forecasting
10%-20%	Good forecasting
20%-50%	Reasonable forecasting
>50%	Weak and inaccurate forecasting

Wave Transformation Analysis

Theoretical wave analysis starts by calculating wavelength, shoaling, and refraction, then creating refraction diagrams and orthogonal wave lines as reference points for reviewing wave modeling. The wave transformation equation is formulated as follows.

$$H' = Ks.Kr.H_0$$

H' is wave height (m), Ks is shoaling coefficient, Kr is refraction coefficient, and H_0 is deep water wave height.

Refraction coefficient:

$$Kr=\sqrt{\frac{b_0}{b}}=\sqrt{\frac{\text{Cos } a_0}{\text{Cos } a_1}}$$

Where the shoaling coefficient is a function of wavelength and water depth.

$$Ks=\sqrt{\frac{n_0\,.\,C_0}{n1\,.\,L1}}$$

Wave refraction occurs in transitional and shallow water depths because wave celerity decreases with decreasing water depths, causing the portion of the wave crest in more surface water to propagate forward at a slower speed than the portion in deeper water. The result is bending the wave crests to approach the bottom contours' orientation. To remain normal to the wave crest, the wave orthogonal will also turn so that the orthogonal parallel in deep water may converge or diverge as wave refraction occurs. This convergence or divergence of wave orthogonal will cause local increases or decreases in wave energy and, consequently, wave height (Sorensen, 2006). Use Crest to make wave refraction patterns (Johnson et al., 1948).

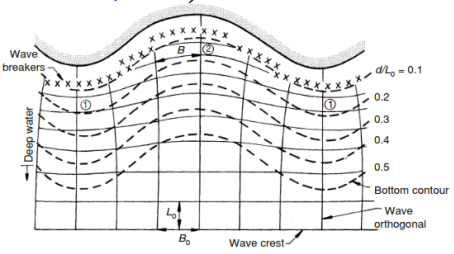

Figure 3. Wave refraction pattern

3. RESULT AND DISCUSSION

Based on wave data for one year (2020) from ECMWF, the dominant waves are from the west (Figure 4.) For deep water, significant wave height data (Hs) and wave period (Ts) used in the analysis and modeling are 0.5 m and 4.2 s. This value was obtained from an average of significant wave hourly data for one month (December 2020) to adjust to the timing of tidal and current measurements at the location so that the modeling results are close to field conditions. The meshing area is modeled using bathymetric data, creating a boundary layer.

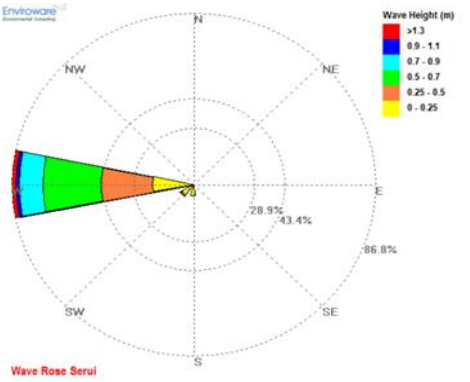

Figure 4. Waverose Serui Jan-Dec 2020

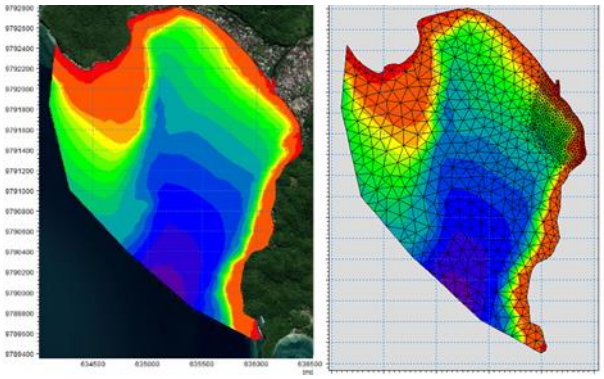

Figure 5. Bathimetri and meshing model

The simulation time used is 15 days for the HD Model and SW Model with 360 timesteps with an interval of 3600 seconds with Eddy viscosity type Smagorinski formulation with a constant value of 0.28 bed resistance type manning number constant 40 $m^{1/3}/s$

Modeling Simulation

Modeling starts from tidal validation to obtain a suitable model in the field by comparing tidal data from HD simulations with tidal observation data at the location. The validation results obtained a MAPE value of 0.3%. Figure 6 shows the validation results between modeling results and field measurements, which can be concluded that tidal modeling is highly accurate forecasting because the difference between tidal measurement data and modeling is petite. It is also shown that the highest and lowest low tides are at the 67th timestep at 19:00 and the 49th timestep at 01:00 on December 15, 2020. These two conditions will be used as a reference in modeling.

Current speed data from field measurements using an ADCP (Acoustic Doppler Current Profiler) placed close to existing coastal protection structures were measured for 293 hours from December 13, 2020, at 14:00 to December 25, 2020, at 18:00. While the graphic comparison of flow speed data from measurement results with modeling results can be seen in Figure 7.

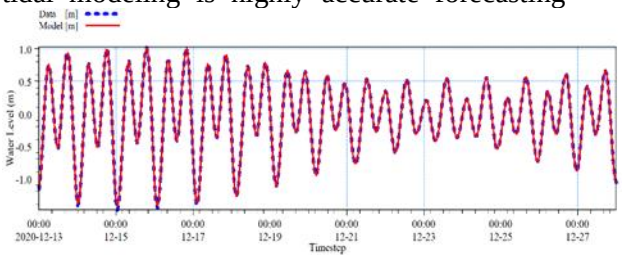

Figure 6. Tide validation

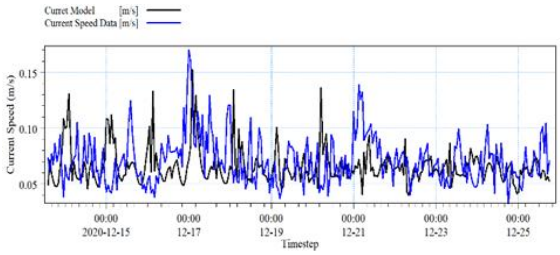

Figure 7. Current speed validation

The validation results obtained a MAPE value of 30%, which is in the reasonable forecasting category. Then, we can continue wave modeling with the Spectral Wave (SW.) Module to see wave propagation and transformation patterns down to the shoreline.

Based on the picture above, there is a change in wave height and wave propagation from deep sea to shallow water, especially in several parts where there are shallow areas before the wave reaches the shoreline on the northeast side of the Serui Fuel Terminal.

Wave Transformation Analysis and Modelling Validation

To determine the accuracy of wave

modeling, theoretical wave calculations are then carried out, and the results of the calculations and orthogonal waves are created, where nine orthogonal waves are divided into two typical (Figure 11). The first is an orthogonal line that passes through a shallow area before heading to the shoreline. The second is straight from deep waters to the shore.

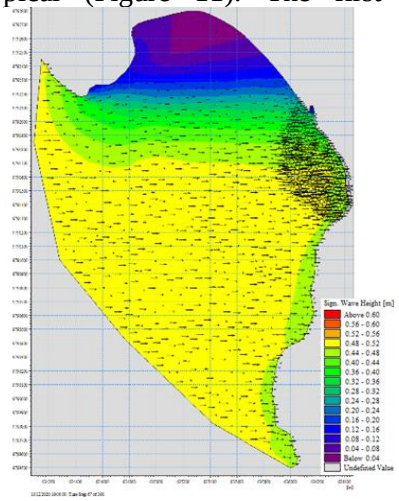

Figure 8. Wave height from west

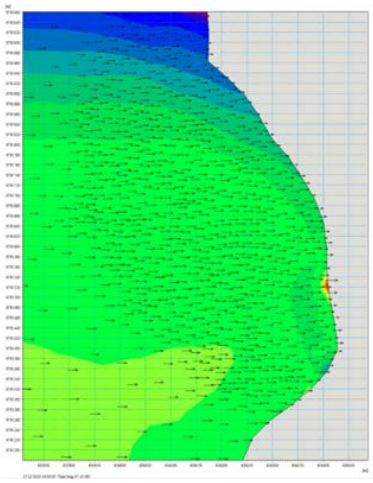

Figure 9. Process of refraction of waves toward the shoreline

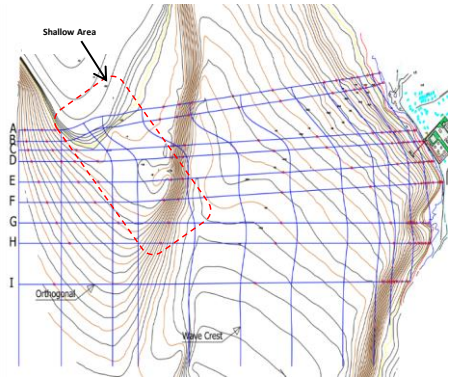

Figure 10. Wave pattern and orthogonal in fuel Terminal Serui

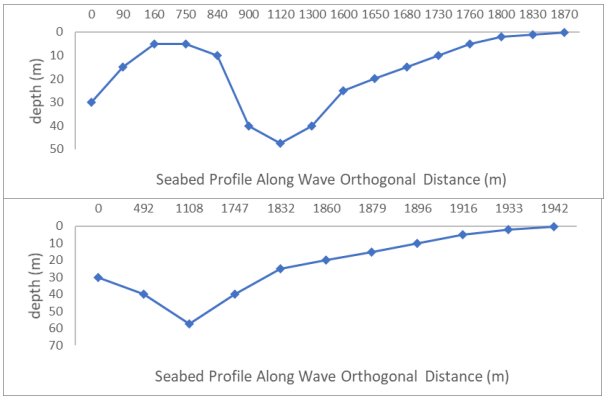

Figure 11. Section profile along orthogonal

The results of calculating wave transformation with an orthogonal line that passes through a shallow area before heading to the shoreline can be seen in Table 3.

Based on the results of the wave transformation analysis, there is a change in wave height for high tide conditions, which for modeling is 0.29 m and for theoretical analysis is 0.25 m with a MAPE value of 7.5%. Meanwhile, the modeling wave height value for low tide conditions is 0.12 m. For theoretical analysis, it is 0.11 m with a MAPE value of 14.0%, which is still included in the good forecasting category. The graph of wave height versus depth is as follows.

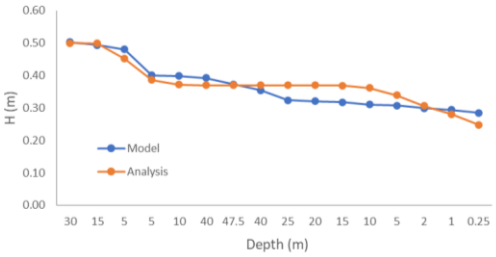

Figure 12. Wave height vs depth through a shallow area (high tide conditions)

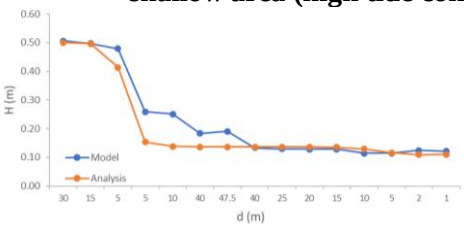

Figure 13. Wave height vs depth through a shallow area (low tide conditions)

Table 3. Wave modeling validation through a shallow area (high and low tide conditions)

Point	Distance	Depth	Hs		MAPE
			Model	Analysis	
Point1	0	30	0.5	0.5	0.01
Point2	90	15	0.49	0.5	0.01
Point3	160	5	0.48	0.45	0.06
Point4	750	5	0.4	0.39	0.04
Point5	840	10	0.4	0.37	0.07
Point6	900	40	0.39	0.37	0.06
Point7	1120	47.5	0.37	0.37	0.01
Point8	1300	40	0.35	0.37	0.04
Point9	1600	25	0.32	0.37	0.14
Point10	1650	20	0.32	0.37	0.15
Point11	1680	15	0.32	0.37	0.16
Point12	1730	10	0.31	0.36	0.16
Point13	1760	5	0.31	0.34	0.1
Point14	1800	2	0.3	0.31	0.02
Point15	1830	1	0.29	0.28	0.05
Point16	1870	0.25	0.29	0.25	0.13
		MAPE			**7.50%**
Point	**Distance**	**Depth**	**Hs**		**MAPE**
			Model	**Analysis**	
Point1	0	30	0.51	0.50	0.01
Point2	90	15	0.50	0.50	0.00
Point3	160	5	0.48	0.41	0.13
Point4	750	5	0.26	0.15	0.41
Point5	840	10	0.25	0.14	0.45
Point6	900	40	0.18	0.14	0.26
Point7	1120	47.5	0.19	0.14	0.29
Point8	1300	40	0.13	0.14	0.02
Point9	1600	25	0.13	0.14	0.05
Point10	1650	20	0.13	0.14	0.06
Point11	1680	15	0.13	0.14	0.05
Point12	1730	10	0.11	0.13	0.13
Point13	1760	5	0.11	0.12	0.02
Point14	1800	2	0.12	0.11	0.12
Point15	1830	1	0.12	0.11	0.09
		MAPE			**14.0%**

Figures 12 and 13 show a significant decrease in wave height in shallow areas, and then in relatively deep waters, there is no change in wave height until it approaches the shoreline, when the wave decreases again. Furthermore, the results of calculating wave transformation with an orthogonal line straight from deep waters to the coastline can be seen in the following Table 4.

The wave height change is insignificant based on the wave transformation analysis result above. The difference in wave height for high tide conditions, which for modeling is 0.46 m and theoretical analysis is 0.41 m with a MAPE value of 2.9%. Meanwhile, the modeling wave height value for low tide conditions is 0.47 m. For theoretical analysis, it is 0.42 m with a MAPE value of 2.9%, which is still included in the highly accurate forecasting category. The graph of wave height versus depth is as follows.

Table 4. Wave modeling validation straight from deep waters to the shoreline (high and low tide conditions)

Point	Distance	Depth	H		MAPE
			Model	Analysis	
Point1	0	40	0.51	0.50	0.02
Point2	1081	65	0.51	0.50	0.01
Point3	1771	40	0.50	0.50	0.00
Point4	1795	30	0.50	0.50	0.00
Point5	1806	25	0.48	0.50	0.03
Point6	1817	20	0.48	0.50	0.03
Point7	1829	15	0.48	0.50	0.03
Point8	1845	10	0.48	0.49	0.02
Point9	1872	5	0.47	0.46	0.02
Point10	1900	2	0.46	0.41	0.11
		MAPE			**2.9%**

Point	Distance	Depth	H		MAPE
			Model	Analysis	
Point1	0	40	0.50	0.50	0.00
Point2	1081	65	0.50	0.50	0.00
Point3	1771	40	0.50	0.50	0.00
Point4	1795	30	0.50	0.50	0.00
Point5	1806	25	0.48	0.50	0.04
Point6	1817	20	0.48	0.50	0.03
Point7	1829	15	0.48	0.50	0.03
Point8	1845	10	0.48	0.48	0.01
Point9	1872	5	0.47	0.44	0.06
Point10	1900	2	0.47	0.42	0.11
		MAPE			**2.9%**

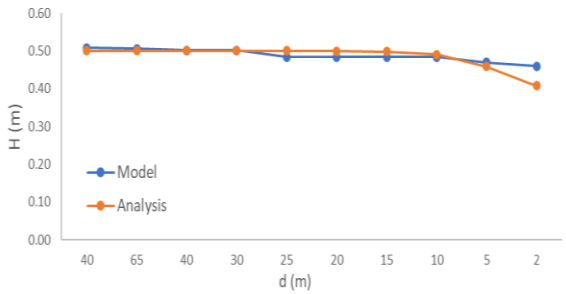

Figure 14. Wave height vs depth straight from deep waters to the shoreline (high tide conditions)

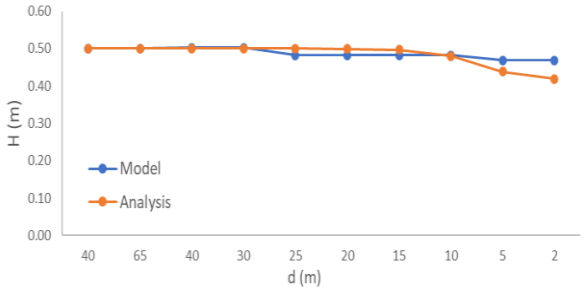

Figure 15. Wave height vs depth straight from deep waters to the shoreline (low tide conditions)

This is very different from the conditions of a depth trough in a shallow area, where there is no significant change in wave height in both high and low tide conditions, so the wave height from the deep sea continues to propagate straight to the shoreline. The wave height values on the coastline at each orthogonal can be seen in the following Table 5.

The average wave height of each orthogonal from the modeling results for high tide conditions (timestep 67) is 0.39 m. The theoretical analysis results show 0.34 m, where the difference between the model and analysis is not too big, with the average MAPE from all orthogonal being around 15%. In contrast, the wave height at the shoreline in each orthogonal low tide condition is presented in (Table 6).

The average wave height of each orthogonal from the modeling results for low tide conditions (timestep 49) is 0.33 m, and from the theoretical analysis results, 0.29 m, where the difference between the model and analysis is not too big with the average MAPE from all orthogonal about 15%.

Table 5. Wave height at the shoreline in each orthogonal (high tide condition)

Orthogonal	H		MAPE
	Model	Analysis	(%)
A	0.29	0.25	13
B	0.31	0.24	20
C	0.40	0.34	15
D	0.33	0.29	12
E	0.43	0.33	23
F	0.44	0.34	22
G	0.45	0.38	17
H	0.45	0.44	2
I	0.46	0.41	11
Average	0.39	0.34	15

Table 5. Wave height at the shoreline in each orthogonal (low tide condition)

Orthogonal	H		MAPE
	Model	Analysis	(%)
A	0.12	0.11	9
B	0.09	0.12	37
C	0.25	0.27	6
D	0.44	0.38	13
E	0.27	0.28	3
F	0.42	0.32	23
G	0.40	0.36	9
H	0.49	0.35	28
I	0.47	0.42	11
Average	0.33	0.29	15

It can be concluded that the wave height at the shoreline is more or less the same, especially in the area around existing coastal buildings. To discover whether building geometry is a factor in overtopping, a run-up calculation was carried out using wave data from orthogonal C, D, E, and F, where the orthogonal coastline is in front of the existing beach buildings. Where to calculate wave run-up, the Irribaren value is calculated. The effectiveness of the overtopping reduction decreases with the increasing number of Iribarren (Kerpen et al., 2019).

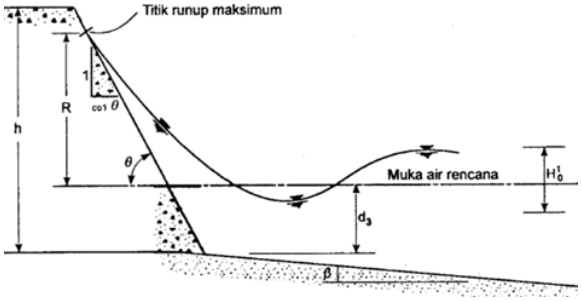

Figure 16. Wave run-up

Various researches have been carried out to calculate run-up. The results of this research are in the form of graphs that can be used for run-up (Triatmodjo, 2011). It has the following form as a function of the Irribaren number for various layers of protection.

$$Ir = \frac{tg\theta}{(\frac{H}{L_0})^{0.5}}$$

Ir is the Irribaren number, θ is the angle of slope of the side of the coastal building, *H* is the wave height at the building location, and L_0 is the wavelength in the deep sea.

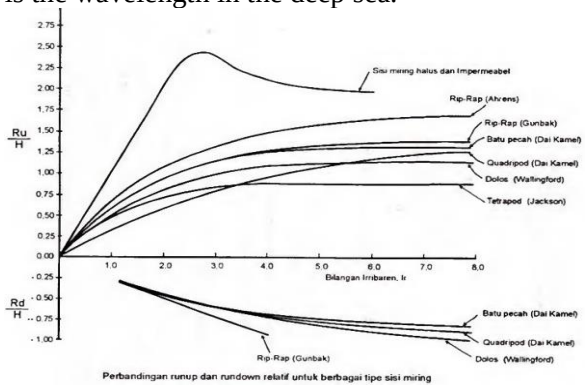

Figure 17. Wave run-up graph

Run-up calculations are only carried out in high tide conditions, which are the conditions with the most significant potential for overtopping. The run-up calculation uses wave height from numerical analysis and modeling results (Tables 7 and 8).

Table 6. Run-up calculation using H Analysis

Orthogonal	Lo	tan θ	Ir	Ru/H	H	Ru
C	21.07	0.63	4.94	2.0	0.34	0.67
D	21.07	0.63	5.32	1.9	0.29	0.55
E	21.07	0.63	5.02	2.0	0.33	0.65
F	21.07	0.63	4.90	2.0	0.34	0.69
Average					0.3	0.6

Table 7. Run-up calculation using the H Model

Orthogonal	Lo	tan θ	Ir	Ru/H	H	Ru
C	21.07	0.63	4.55	2.0	0.40	0.80
D	21.07	0.63	4.99	2.0	0.33	0.66
E	21.07	0.63	4.39	2.1	0.43	0.90
F	21.07	0.63	4.33	2.1	0.44	0.92
Average					0.4	0.8

From the results of run-up calculations with a wave height of 0.3-0.4 m, the run-up height is in the range of 0.6 – 0.8 m. It can be concluded that the building structure doubles the wave height when it creeps into existing coastal buildings. Figure 16. illustrates the run-up height when a wave approaches the coastal structure of waves on existing coastal buildings.

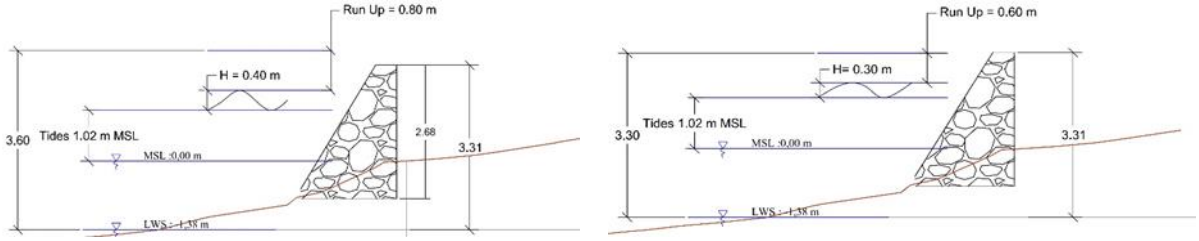

Figure 18. Run-up when a wave approaches existing coastal buildings

4. CONCLUSION

Hydrodynamic modeling simulation, where validation of tidal modeling and field measurement results has a MAPE value of 0.3%, which is included in the highly accurate forecasting category, as well as for current modeling, where validation of current speed modeling and field measurement results has a MAPE value of 30% which is included in the reasonable forecasting category.

Then, for wave modeling with theoretical analysis at each orthogonal, an average MAPE value of 15% is obtained, which is in the good forecasting category. The modeling result for high tide conditions (timestep 67) is 0.39 m, and from the theoretical analysis, the result is 0.34 m. Then, for low tide conditions (timestep 49), it is 0.33 m, and from the theoretical analysis results, 0.29 m, where the difference between the model and analysis is not too big with

For the wave modeling with theoretical analysis at each orthogonal, an average MAPE value of 15% is obtained, which is in the good forecasting category. The modeling results for high tide conditions (timestep 67) are 0.39 m, and from the theoretical analysis, the results are 0.34 m. Then, for low tide conditions (timestep 49), it is 0.33 m, and from the theoretical analysis results, 0.29 m, where the difference between the model and analysis is not too big with

In general, the wave height in the waters of the Serui fuel terminal is around 0.3-0.4 m, where the waves are relatively calm, and the cause of the overtopping that occurs is due to the geometry and type of existing coastal buildings with smooth sloping sides and impermeable which makes the wave height double with a run-up height 0.6-0.8 m

It should be noted that the significant sea wave height (Hs) used in wave modeling and run-up analysis was obtained from important wave data for one month (December 2020), where the wave height that occurred could be greater than the modeling and analysis in this research. So, before deciding on alternative solutions, whether new buildings or modifications to existing buildings, further research needs to be carried out using optimal wave return period data.

REFERENCES

Amalia, R., Atmodjo, W., Purwanto. (2014). Studi Refraksi dan difraksi gelombang pada rencana bangunan pelabuhan di Tanjung Bonang, Kabupaten Rembang. *Journal Oseanografi*, 3(4): 582–588.

Belibassakis, K.A., Athanassoulis, G.A., Gerostathis, T.P. (2014). Directional wave spectrum

transformation in the presence of strong depth and current inhomogeneities by means of coupled-mode model. *Ocean Engineering*, 87:84–96.

CERC. (1984). *Shore protection manual: Vol. I* (IV). US Army Coastal Engineer Research Center.

DHI. (2014). *Spectral wave module scientific documentation*. www.mikebydhi.com

Di Leo, A., Dentale, F., Buccino, M., Tuozzo, S., Pugliese Carratelli, E. (2022). Numerical analysis of wind effect on wave overtopping on a vertical seawall. *Water (Switzerland)*, 14(23).

Fang, K.Z., Yin, J.W., Liu, Z.B., Sun, J.W., Zou, Z.L. (2014). Revisiting study on Boussinesq modelling of wave transformation over various reef profiles. *Water Science and Engineering*, 7(3): 306–318.

Ghipari, A., Suntoyo, S., Armono, H.D. (2012). Pemodelan perubahan morfologi pantai akibat pengaruh submerged breakwater berjenjang. *POMITS*, 1(1): 1–6.

Husrin, S., Prihantono, J. (2007). Simulasi kondisi hidro-oseanografi perairan Yapen-Worepen Teluk Cendrawasih Propinsi Papua. *Jurnal Segara*, 3(2): 81–96.

Johnson, J.W., O'Brien, M.P., Isaacs, J.D. (1948). *Graphical Construction of wave refraction diagrams*. US Navy Hydrographic Office.

Kerpen, N.B., Schoonees, T., Schlurmann, T. (2019). Wave overtopping of stepped revetments. *Water (Switzerland)*, 11(5).

Lewis, C.D. (1982). *Industrial and business forecasting methods : a practical guide to exponential smoothing and curve fitting*. Butterworth Scientific.

Mandlier, P.G., Kench, P.S. (2012). Analytical modelling of wave refraction and convergence on coral reef platforms: Implications for island formation and stability. *Geomorphology*, 159–160: 84–92.

Oliveira, J.N.C., Oliveira, F.S.B.F., Trigo-Teixeira, A.A. (2018). Modelling the beach morphodynamics in defence schemes of combined groyne fields and seawalls under storm conditions. *5as Jornadas de Engenharia Hidrográfica*.

Pratikto, W.A., Suntoyo, S., Solikhin, S., Sambodho, K. (2014). *Struktur pelindung pantai*. PT. Media Saptakarya.

Rusu, E., Gonçalves, M., Guedes Soares, C. (2011). Evaluation of the wave transformation in an open bay with two spectral models. *Ocean Engineering*, 38(16): 1763–1781.

Sorensen, R.M. (2006). *Basic coastal engineering*. Springer Science+Business Media.

Sugianto, D.N., Andika, B.C. (2015). Transformasi gelombang untuk perencanaan pelabuhan hubungan internasional. *Ilmu Kelautan: Indonesian Journal of Marine Sciences*, 20(1): 9–22.

Taylor-Burns, R., Nederhoff, K., Lacy, J.R., Barnard, P.L. (2023). The influence of vegetated marshes on wave transformation in sheltered estuaries. *Coastal Engineering*, 184.

Triatmodjo, B. (2011). *Perencanaan bangunan pantai*. Beta Offset.

Van Der Werf, I.M., Van Gent, M.R.A. (2018). Wave overtopping over coastal structures with oblique wind and swell waves. *Journal of Marine Science and Engineering*, 6(4).